STRUCTURAL DESIGN AND EXPERIMENTAL ANALYSIS OF NEW PIPELINE REPAIR EQUIPMENT

Yong CHEN[1,2], Ding YANG[1], Zheng ZHANG[1], Dongying MENG[3]

In response to the problem of the existing pipeline repair equipment being cumbersome to operate, having large errors, and being unable to guarantee a successful cut and dock in one go, this paper carries out the structural design and experimental analysis of new type of pipeline repair equipment. The structural design of the new pipeline repair equipment has the technical advantages of accurately finding the center inside the pipeline, achieving laser alignment at a long distance and with high precision, and quickly marking lines. The structural design is further elaborated from three aspects: the establishment of the theoretical model, the calculation of the structural parameters, and the finite element analysis of the parameters of the key components. This paper believes that for two DN400 pipelines with non-overlapping axes and an axis inclination angle within 10°, when the connecting rod length is designed to be 190mm, the design of the key components conforms to the equal life design principle, and the maximum load received by the key components does not exceed the material yield limit. Experimental results demonstrate that, after familiarizing oneself with the installation and usage procedures of the new pipeline repair equipment, The equipment's fixation work, long-distance alignment work and line drawing work can be completed within 5 minutes. and the error does not exceed 2mm. Both the marking lines time and the precision of the cutting butt joint meet field operation requirements. The findings of this paper can provide significant technical support for the design of long-distance pipeline repair equipment.

Keywords: Long-distance pipeline; New pipeline repair equipment; Structural design; Finite element analysis; Experiment

[1] School of Mechatronic Engineering, Southwest Petroleum University, No. 8, Xindu Avenue, Chengdu 610500, China. e-mail address:swpucy1412@163.com. (corresponding author)

[2] Oil and Gas equipment technology Sharing and Service Platform of Sichuan Province.

[3] Gas Transmission Management Department of PetroChina Southwest Oil and Gasfield Company,Chengdu,China.

1. Introduction

The technology of pipeline cutting and alignmenting was developed in response to the need for sealing and connecting pipelines during the construction of medium to long-distance pipelines[1-3]. Welding deformation causes the axes of the two connected pipeline sections to misalign at the connection point, resulting in varying degrees of circumferential displacement. This necessitates the use of a cutting machine to make oblique cuts in the steel pipe to compensate for the misalignment[4-6] . Additionally, as the pipeline system ages, local sections may need to be replaced due to factors such as corrosion and third-party damage, which can cause pipeline deformation and leakage. However, once a buried pipeline is severed, various stresses are released, causing displacement at the pipe ends[7]. The space between the pipe ends cannot be filled with a standard cylindrical pipe section. This led to the development of the pipeline cutting and docking technology[8-10].

The China National Petroleum Corporation (CNPC) currently utilizes three types of pipeline repair equipment: steel pipeline cutters, pipeline scribes, and quick connectors[11-13]. They have applied for and received patent authorization for these. In the early stages, foreign countries primarily employed large-scale excavation methods. Later, they mostly used lofting methods for manual calculations, followed by cutting with STZQ-I type pipe cutting machines. However, the technology of pipeline cutting and docking that most pipeline construction units currently use has significant drawbacks[14]. The cutting process is not only cumbersome and time-consuming, but it also requires manual measurements of the up, down, left, right, and deviation angles of the pipe section that needs to be replaced. Furthermore, complex calculations are needed to obtain the cutting parameters[15]. The cumulative error is so large that it is impossible to meet the pipe replacement requirements in a single attempt.

Therefore, in the field of pipeline cutting and docking, there is an urgent need for a pipeline repair equipment that is easy to operate, highly accurate, can complete the docking and marking lines work within 5 minutes, and can guarantee to meet the pipe replacement requirements in one go. Based on the aforementioned research, this paper proposes a new type of pipeline repair equipment. Finite element methods are used to perform parameter analysis on key components. Through group comparison, the optimal structural scheme is obtained. Finally, field experiments on working principles and reliability are conducted.

2. Conduct research on the structural design of new type of pipeline cutter.

2.1 Establish a theoretical model for new pipe docking

The selected pipe diameter for the model construction is DN400, with a wall thickness of H. A situation where the axes of the two end pipes do not coincide is chosen. A point O_1 is taken on the axis of the left end pipe A_1, and a point O_2 is taken on the axis of the right end pipe A_2, and the two points O_1 and O_2 are connected. The left end pipe A_1 is cut through the point O_1 and perpendicular to the plane of the line segment O_1O_2 to obtain the elliptical surface B_1, and the left end pipe A_2 is cut through the point O_2 and perpendicular to the plane of the line segment O_1O_2 to obtain the elliptical surface B_2. A DN400 pipe A_3 for replacement is taken, the length of the pipe A_3 is the same as the line segment O_1O_2, the axis of the pipe A_3 coincides with O_1O_2, and the two end faces of the pipe A_3 are docked with the elliptical surfaces B_1 and B_2, completing the pipe docking work, as shown in Fig. 1(a).

The axes of pipelines A_2 and A_3 have a deflection angle of θ. The DN400 pipeline has an outer diameter of Φ_1 and an inner diameter of Φ_2. As illustrated in Fig. 1(b), this allows us to derive the following formula:

$$CE2 = \frac{\Phi_1}{COS\theta} \tag{1}$$

$$CD2 = \frac{\Phi_1+\Phi_2}{2COS\theta} \tag{2}$$

Both the outer and inner walls of end face B_2 are elliptical, Misalignment occurs at the docking point on the long axis of the ellipse between end faces B_2 and B_3, as depicted in Fig. 1(b). The minimum wall thickness at the docking point between end faces B_2 and B_3 is H_{min}.

$$Hmin = \frac{\Phi_1}{2} - \frac{\Phi_2}{2COS\theta} \tag{3}$$

Given that H=13mm, Φ_1=406mm, Φ_2=380mm, and θ=10º, substituting these values into formula (3) yields H_{min}=10.07mm. Since the docking point requires a welding process for connection, any change in wall thickness at the docking point due to diameter variation when cutting the pipe section can be disregarded, provided the welding thickness exceeds 2.93mm.

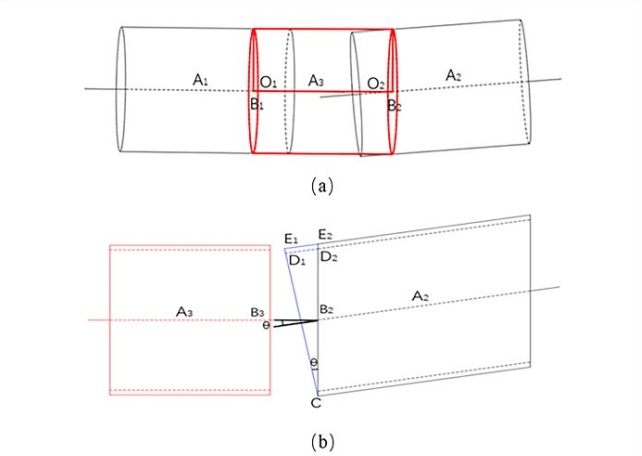

Fig. 1. Model of pipe docking

2.2 Structural design of new pipe repair equipment

Based on the established theoretical model, this paper designs a new pipeline repair equipment. This structural design has the functions of accurately finding the centering inside the pipeline, long-distance high-precision laser alignment, and quickly marking lines, as shown in Fig. 2. The new pipeline repair equipment is composed of three structural parts, namely the support structure, as shown in Fig. 2(a); the deflection structure, as shown in Fig. 2(b); and the line drawing structure, as shown in Fig. 2(c).

The working principle of the new pipeline repair equipment is as follows: First is the support structure, by rotating the trapezoidal threaded rod, the trapezoidal threaded rod is connected to the threaded sleeve through the trapezoidal thread, and the threaded sleeve will move left and right along the direction of the guide rod. The threaded sleeve is connected to four sets of connecting rods through bolts, and the move of the threaded sleeve will drive the connecting rods to synchronously press the four support plates against the inner wall of the pipeline to complete the support and fixation. Next is the deflection structure, the centering disc and the deflection ring can rotate relative to each other on the vertical axis, and the deflection ring and the mounting base can rotate relative to each other on the horizontal axis. The deflection structure can realize rotation in any direction in space through the deflection ring and the centering disc, enabling the laser emitter to adjust the deflection angle arbitrarily for long-distance laser alignment. Finally is the line drawing structure, the marking pen connected to the marking bracket can rotate 360 degrees around the axis of the laser emitter, to achieve the marking pen drawing an elliptical trajectory that can be connected at the beginning and end on

the outer wall of the pipeline that needs to be repaired.

The specific operation process is as follows: The new pipeline repair equipment needs to be used in pairs, as shown in Fig. 2(d). The transmitting end and the receiving end complete the support and fixation on the inner wall of the pipeline through the support structure. The laser pen at the transmitting end emits a laser, which can deflect at any angle in space through the deflection structure, aiming the laser at the center of the centering disc at the receiving end. Finally, it's the line drawing structure, the marking pen rotates around the outer wall of the pipeline at the transmitting end to draw a line. This completes the line drawing work at the transmitting end of the pipeline. Then, the laser emitter and the line drawing structure are disassembled from the transmitting end and installed at the receiving end, repeating the laser alignment and line drawing of the transmitting end, completing the line drawing work at the receiving end of the pipeline.

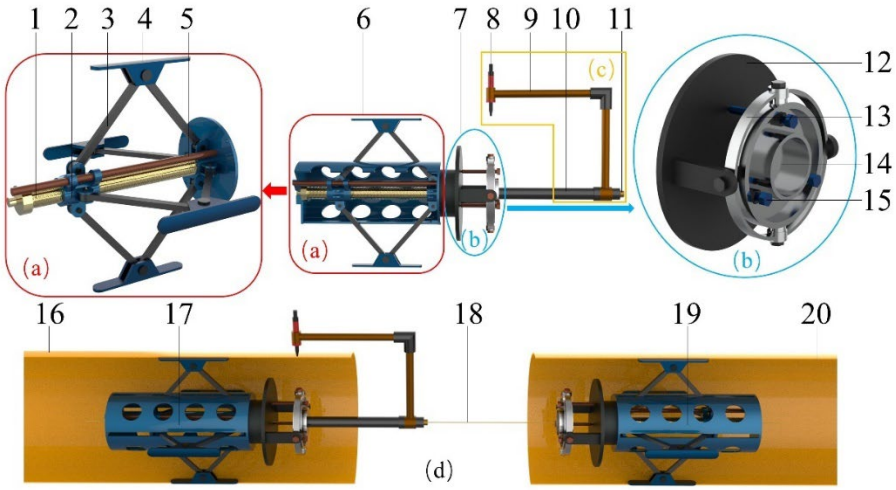

1—Trapezoidal threaded rod; 2—Threaded sleeve; 3—Connecting rod; 4—Support plate; 5—Guide rod; 6—Deflection structure; 7—Deflection structure; 8—Marking pen; 9—Marking bracket; 10—laser emitter; 11—Laser pen; 12—Mounting base; 13—Deflection ring; 14—Centering disc; 15—Retaining bolt; 16—Pipeline; 17—The transmitting end; 18-Laser; 19—The receiving end; 20—Pipeline

Fig. 2. Schematic diagram of working principle

2.3 Specific structural parameters of new pipe repair equipment

Upon completion of its fixation within the pipe, the new pipeline repair equipment, using the support plate as a reference, is divided into two parts: left and right. The weight of the left side is M_1, while the right side is M_2. The new pipeline

repair equipment is simplified into a homogeneous slender rod of equivalent weight, resulting in a force analysis diagram of the entire equipment, as shown in Fig. 3(a). Forces G_1 and G_2 represent gravity, while forces Ff_1 and Ff_2 represent the frictional forces between the support plate and the inner wall of the pipe. Given that the four support plates open synchronously, the frictional forces Ff_1 and Ff_2 are equal. There are two support plates at the position corresponding to force Ff_2, with g being the gravitational coefficient.

List the equilibrium equations：

$$G_1 \times \frac{a}{2} + Ff_1 \times 2c + Ff_2 \times 2c = G_2 \times \frac{b}{2} \tag{4}$$

$$G_1 + G_2 = F_1 \tag{5}$$

Given that G_1=78.4N,G_2=156.8N,a=235mm, b=470mm, c=180mm, and g=9.8N/Kg. Substituting these values into the formulas(4) and (5), we get Ff_1= Ff_2=38.38N, and F1=235.2N. When the friction force between a single support plate and the inner wall of the pipe is 38.38N, the new pipe repair equipment achieves static equilibrium when fixed inside the pipe. The friction coefficient between the support plate and the inner wall of the pipe is taken as μ=0.15, and the squeezing force of the support plate on the inner wall of the pipe is F_j=255.87N. As the lowermost connecting rod has to bear the entire weight of the equipment, it experiences the largest force, which is 491.07 N. The safety working parameter S is defined as 1.5. This paper posits that in actual work, after the new pipe repair equipment is fixed inside the pipe, the force on the lowermost connecting rod is 736.605 N, and the force on the other three groups of connecting rods is 383.805N.

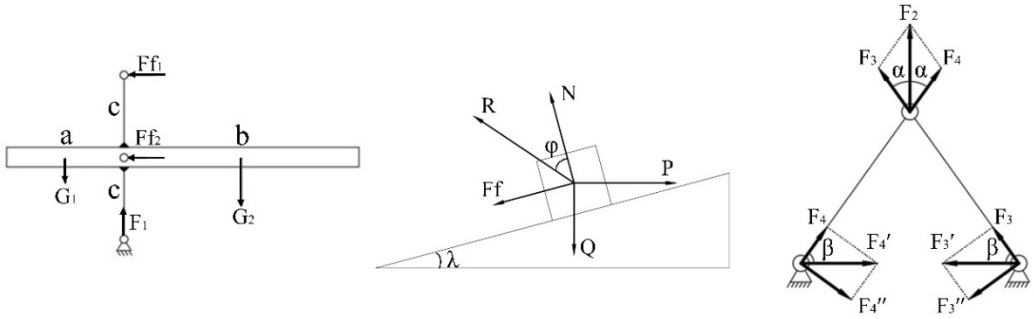

Fig. 3. Mechanical model sketch

The connection method of the trapezoidal threaded rod and the threaded sleeve is thread connection. Analyze the relationship between the input torque of the trapezoidal threaded rod and the axial thrust received by the threaded sleeve.

The input torque M of the trapezoidal threaded rod is equal to the product of the tangential force P and half of the diameter d_2 of the trapezoidal threaded rod：

$$M = P \times \frac{d_2}{2} \quad (6)$$

The movement of the threaded sleeve and the trapezoidal threaded rod can be seen as a small slider moving upward on a slope with an angle of λ, being pulled by P. λ is the helix angle, Q is the pressure received by the threaded sleeve, which is also the lifting force of the threaded sleeve, N is the support force of the trapezoidal threaded rod on the threaded sleeve. Ff is the frictional force received by the threaded sleeve, and R is the resultant force of N and Ff. As shown in Fig.3(b).

The relationship between the input torque of the trapezoidal threaded rod and the axial thrust received by the threaded sleeve is:

$$P = Q \times tan(\lambda + \varphi) \quad (7)$$

$$M = Q \times tan(\lambda + \varphi) \times \frac{d_2}{2} \quad (8)$$

$$Tan(\lambda) = \frac{s}{\pi \times d_2} \quad (9)$$

$$S = K \times t \quad (10)$$

$$Tan(\varphi) = \mu_t = \frac{Ff}{N} \quad (11)$$

$$\Delta = 90° - \frac{\lambda}{2} \quad (12)$$

$$M_t = \frac{\mu}{sin(\delta)} \quad (13)$$

The calculated parameters of the trapezoidal threaded rod are shown in Table 1.

Table 1

Parameter table for the trapezoidal threaded rod

Parameters	λ	δ	K	s	t	μ	d_2	μ_t	φ
Calculated value	15°	82.5°	4	24	6	0.15	28.511	0.1513	8.603°

Based on the calculated parameter values, the relationship formula between the input torque of the trapezoidal threaded rod and the axial thrust received by the threaded sleeve is:

$$M = 6.229Q \quad (14)$$

Once the new pipe repair equipment is installed and fixed inside the pipe,

the threaded sleeve connected to the connecting rod can be equivalent to a fixed base. The simplified force analysis diagram of the four sets of connecting rods that perform the support function is shown in Fig. 3(c).

The relationship formula between the support force F_2 of a set of connecting rods and the horizontal component F_3' of force F_3 is:

$$F_3{}' = \frac{F_2}{2cos\alpha cos\beta} \quad (15)$$

When the new pipeline repair equipment is fixed inside the pipeline, the support force of each group of connecting rods is 383.805N. These four groups of support forces are substituted into formula (15) to obtain the horizontal axial force of the connecting rod on the threaded sleeve. The sum of these four horizontal axial forces is equal to the axial thrust Q received by the threaded sleeve. In order to study the relationship between the length of the connecting rod and the input torque of the trapezoidal threaded rod, the value range of the connecting rod length is defined as 160mm~200mm, the increment is 5mm, and 9 groups of connecting rod lengths are set for analysis. As shown in Table 2.

Table 2

Parameter table for different connecting rod lengths

Connecting rod length (mm)	Vertical angle α (°)	Horizontal angle β (°)	Axial thrust Q (N)	Input torque M (N•mm)
160	33.28	56.72	1673.306	10423.359
165	35.84	54.16	1617.186	10073.452
170	38.11	51.89	1580.717	9846.286
175	40.15	49.85	1557.487	9701.587
180	42	48	1543.676	9615.558
185	43.69	46.31	1536.826	9572.889
190	45.25	44.75	1535.278	9563.247
195	46.69	43.31	1537.895	9579.548
200	48.02	41.98	1543.79	9616.268

3. Finite element analysis of critical components

3.1 Material parameters of key components

According to the structural design of the new pipeline repair equipment, establish a three-dimensional model of the support structure. This structure is composed of connecting rods and support plates. Also, establish a three-

dimensional model of the guide structure, which is composed of threaded sleeve and guide rod. In terms of material selection, the materials of the connecting rod, support plate, guide rod, and threaded sleeve are all Q245 steel. The density is 7800kg/m3, the Poisson's ratio is 0.3, and the Young's modulus is 210GPa. The nominal diameter of the pipeline is DN400.

3.2 Establish the three-dimensional finite element model

When the new pipeline repair equipment is in operation, the four key components - connecting rods, support plates, guide rod, and threaded sleeve - are all in a high stress state. To ensure the rationality of the structural design and that the key components are always in a safe state during use, the following operations need to be carried out: (1) Analyze the equivalent stress received by the support structure and guide structure under working conditions through the finite element method. (2) By changing the length parameter of the connecting rod, analyze what value of the connecting rod parameter makes the structural design of the entire new pipeline repair equipment optimal.

The simplified three-dimensional model of the support structure under working conditions consists of the connecting rods, support plate, and bases, while the simplified three-dimensional model of the guide structure under working conditions consists of the guide rod and threaded sleeve. In Abaqus software, the established simplified three-dimensional model of the support structure and the guide structure are divided into grids using structural hexahedral mesh. Taking the length of the connecting rod as 160mm as an example, the finite element mesh models of the established support structure and guide structure are shown in Fig. 4. According to the data of the 9 sets of connecting rod lengths set, 9 corresponding simplified three-dimensional models of the support structure and guide structure are established respectively, and imported into Abaqus software for setting and analysis.

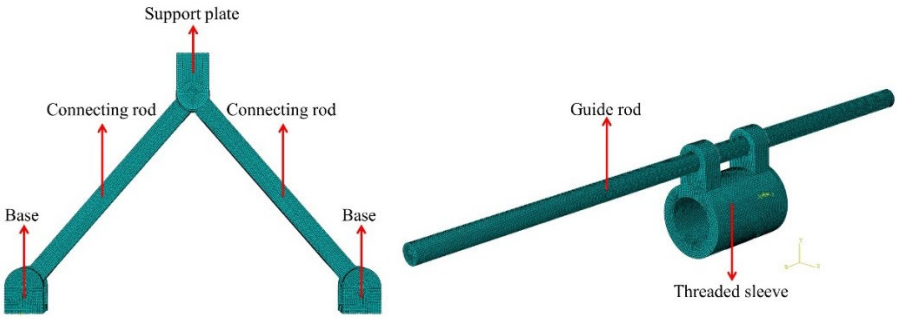

Fig. 4. The finite element grid model

In Abaqus software, fully fixed constraints are applied to the two bases of the support structure, and a uniformly distributed load is applied to the entire surface of the support plate. The size of the load is equal to the maximum squeezing force of the inner wall of the pipeline on the support plate under working conditions, which is 736.605N. Fully fixed constraints are applied to both ends of the guide rod of the guide structure, a node RP-1 is created at the center of the threaded sleeve, and RP-1 is coupled with the threaded sleeve for motion. A rotational torque is applied to RP-1, and the size of the torque is equal to the input torque M. As shown in Fig. 5.

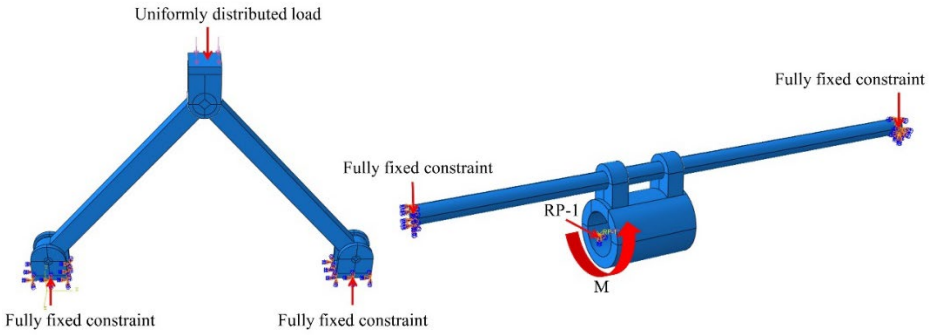

Fig. 5. The setting of boundary conditions

Element independence verification is performed on these two models, as shown in Fig. 6. This figure shows the variation of the maximum equivalent stress of the guide structure and the support structure with the number of elements. When the number of elements of the guide structure is greater than 200,000 and the number of grids of the support structure is greater than 190,000, the calculation results of the model tend to be stable. To ensure the calculation accuracy of this simulation, and to minimize the amount of calculation to maximize the calculation efficiency, this paper finally determines the number of elements of the guide structure to be 222,593 and the number of elements of the support structure to be 191,556. At this time, the element sizes of the support plate, connecting rod, and base are 0.9mm, 0.7mm, and 0.5mm respectively, and the element sizes of the threaded sleeve and guide rod are 0.9mm and 0.7mm respectively. At the same time, there are no warnings in the element quality check.

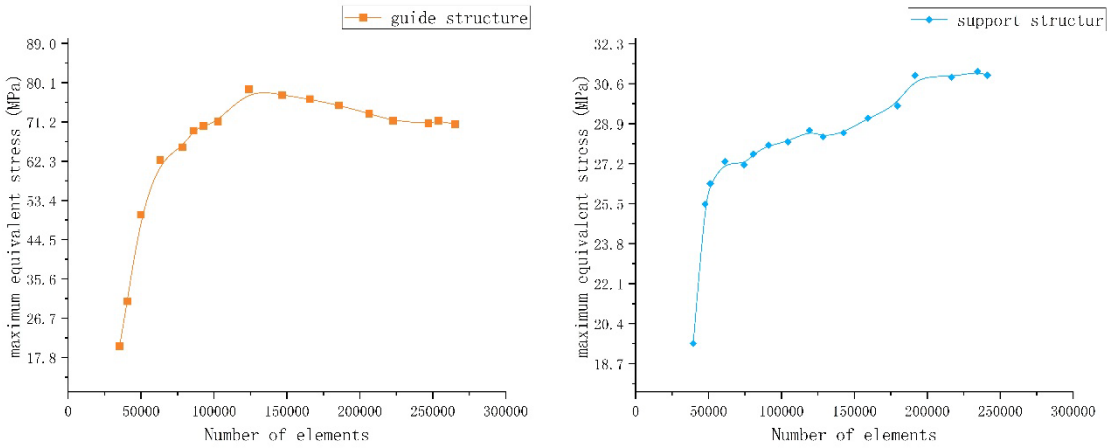

Fig. 6. The element independence verification

3.3 Simulation results of the finite element model

The simulation results are as follows. These are the stress cloud diagrams of the connecting rod, guide rod, and threaded sleeve under different lengths of the connecting rod. In addition, there are also displacement cloud diagrams of the support structure and guide structure under different lengths of the connecting rod.

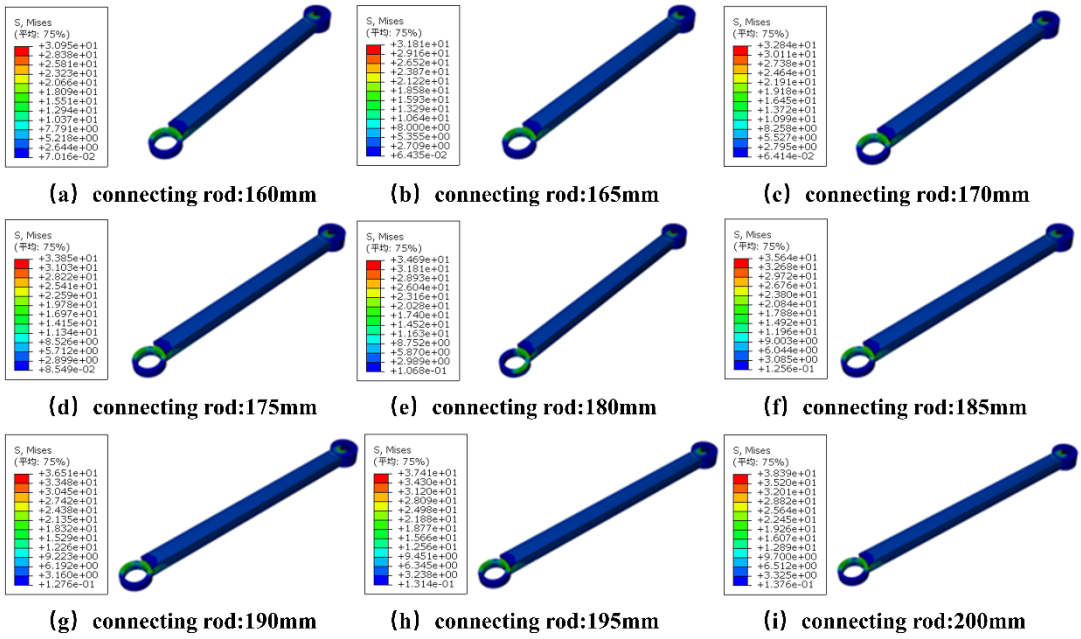

Fig. 7. The stress cloud diagram of the connecting rod

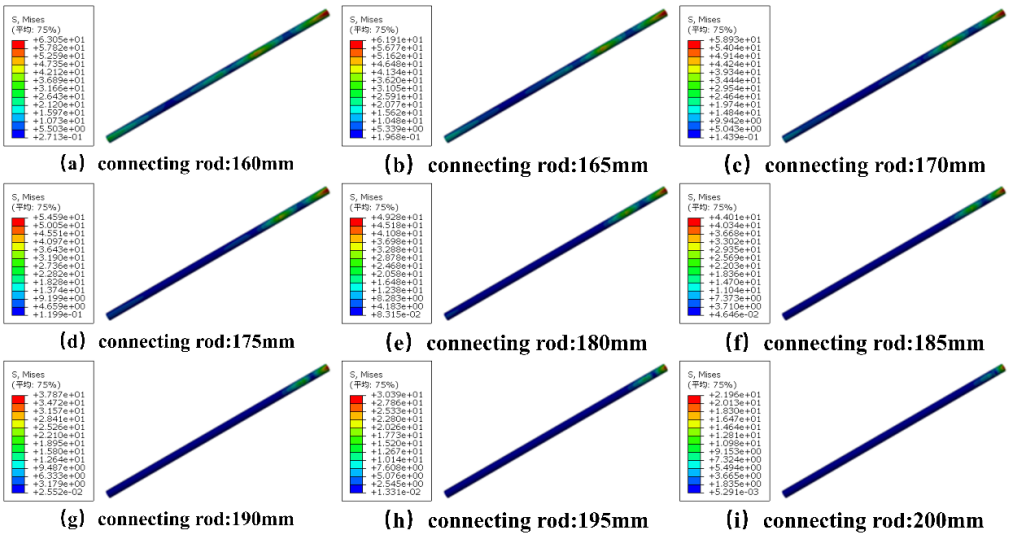

Fig. 8. The stress cloud diagram of the guide rod

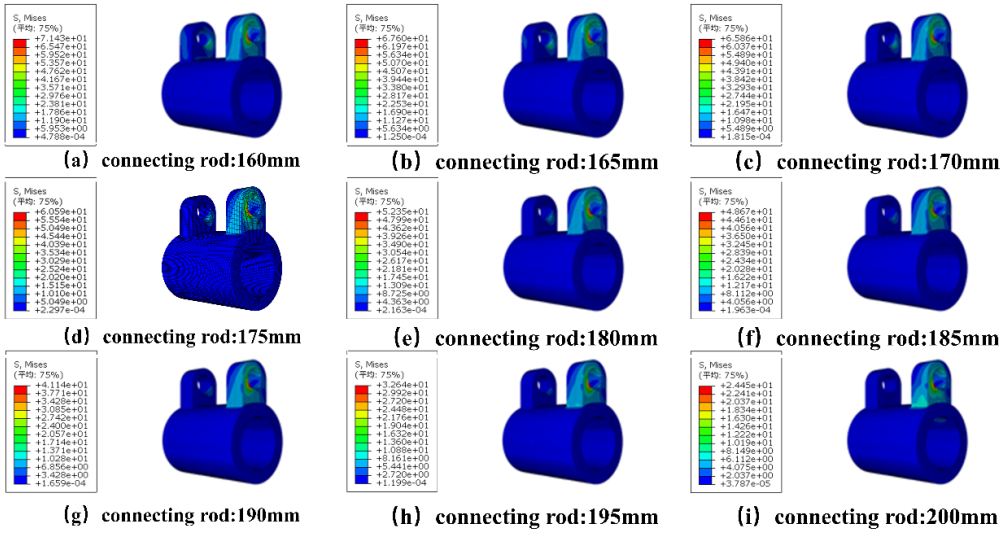

Fig. 9. The stress cloud diagram of the threaded sleeve

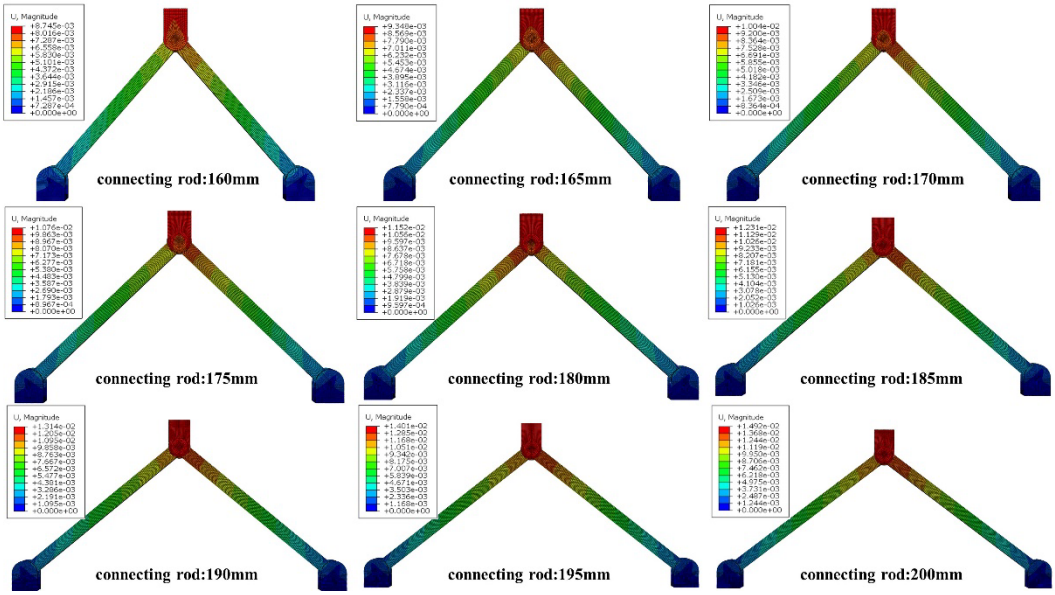

Fig. 10. The displacement cloud diagrams of the support structure

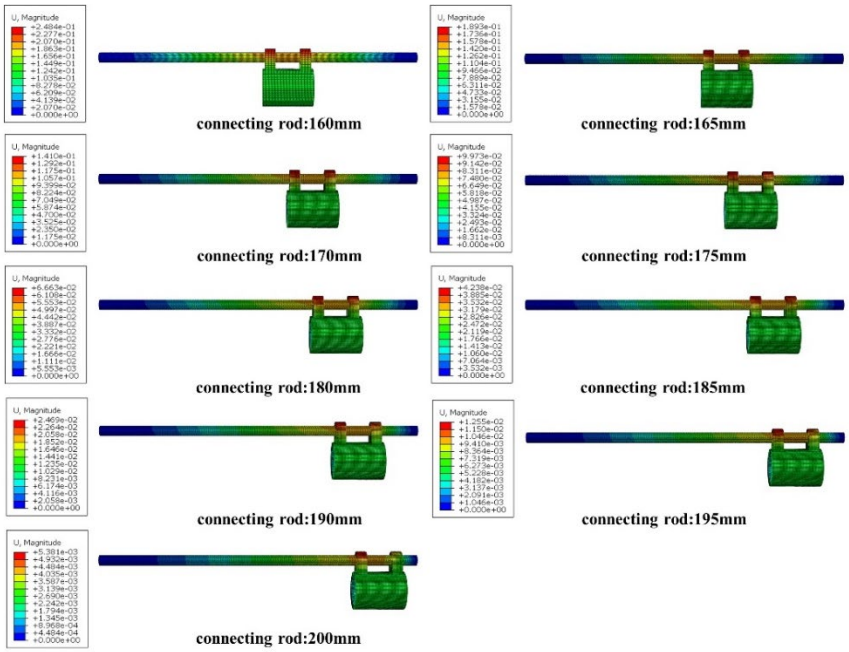

Fig. 11. The displacement cloud diagrams of the guide structure.

By analyzing the displacement cloud diagrams of the support structure and guide structure, it is found that when the length of the connecting rod is less than 195mm, the maximum displacement of the parts occurs on the threaded sleeve part.

Therefore, in most cases, compared with the connecting rod and guide rod, the threaded sleeve is the part that is prone to damage.

By summarizing the simulation data, we obtained the stress summary tables for three components: the connecting rod, the guide rod, and the threaded sleeve, as shown in Table 3.

Table 3

Summary table of simulation data

Connecting rod length[mm]	Connecting rod [MPa]	Guide rod [MPa]	Threaded sleeve [MPa]
160	30.95	63.05	71.43
165	31.81	61.91	67.60
170	32.84	58.93	65.86
175	33.85	54.59	60.59
180	34.69	49.28	52.35
185	35.64	44.01	48.67
190	36.51	37.87	41.14
195	37.41	30.39	32.64
200	38.39	21.96	24.45

3.4 Analyze the simulation results of the finite element model

An analysis of the data in the table reveals that the maximum stress values for the connecting rod, guide rod, and threaded sleeve are 38.39 MPa, 63.05 MPa, and 71.43 MPa, respectively. Given that the yield limit of the Q245 material is 245 MPa, it can be concluded that the stress experienced by these three components does not exceed the yield limit of the Q245 material under any of the nine different connecting rod length parameters.

To gain a more intuitive understanding of the stress variations in the connecting rod, guide rod, and threaded sleeve under different connecting rod length parameters, the data from Table 3-5 is displayed as a line graph. The graph reveals that as the length of the connecting rod increases, the stress experienced by the connecting rod also increases. Conversely, the stress on the guide rod and threaded sleeve decreases with an increase in the length of the connecting rod, as depicted in Fig. 10(a).

In an effort to enhance the overall performance of the structure, facilitate maintenance and replacement, and prevent a single component failure from rendering the entire equipment unusable, this study adopts the equal life design

concept. This approach aims to align the design life of key components as closely as possible. This necessitates that the stresses experienced by the connecting rod, guide rod, and threaded sleeve during operation are as similar as possible. A variance diagram, illustrating the stress experienced by these components under different connecting rod length parameters, is presented in Fig. 10(b). The analysis reveals that when the connecting rod length is set at 190mm, the variance value is minimized. At this point, the design life of the three key components - the connecting rod, guide rod, and threaded sleeve - is most closely aligned. Therefore, a connecting rod length of 190mm is selected as the optimal design parameter for this structure.

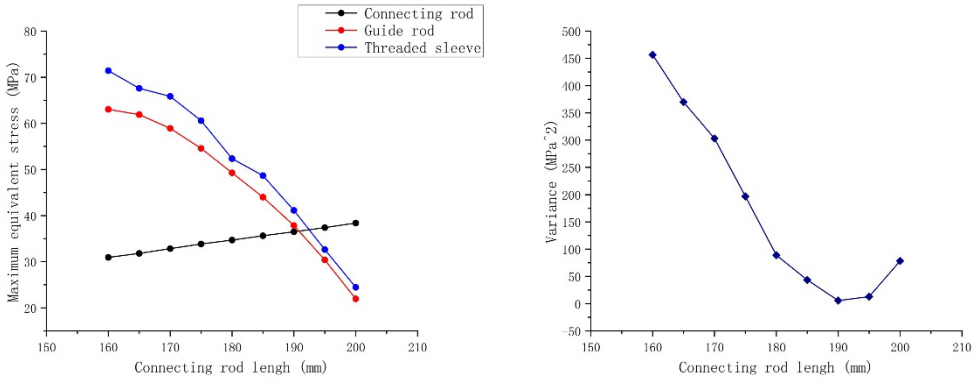

Fig. 12. The maximum equivalent stress and variance graph

4. Conduct experimental analysis on the new pipeline repair equipment.

Follow the operation steps to install the new pipe repair equipment inside the pipe for secure fixation. Once the installation is completed, carry out the laser long-distance alignment, ensuring that the laser is aimed at the expected position. Subsequently, perform the marking work on the outer wall of the pipe, and observe whether the marking lines on the pipe connects from the beginning to the end, as depicted in Fig. 13(a),(b)and(c). Record the operation time, and repeat this operation 5 times. This process is to determine the time required for the entire installation-marking process after the operator transitions from novice to proficient, as illustrated in Table 4. It can be concluded that as the number of operations increases, the operator's speed of using the new pipeline repair equipment becomes faster and faster. It is entirely possible to achieve the goal of completing the marking within 5 minutes

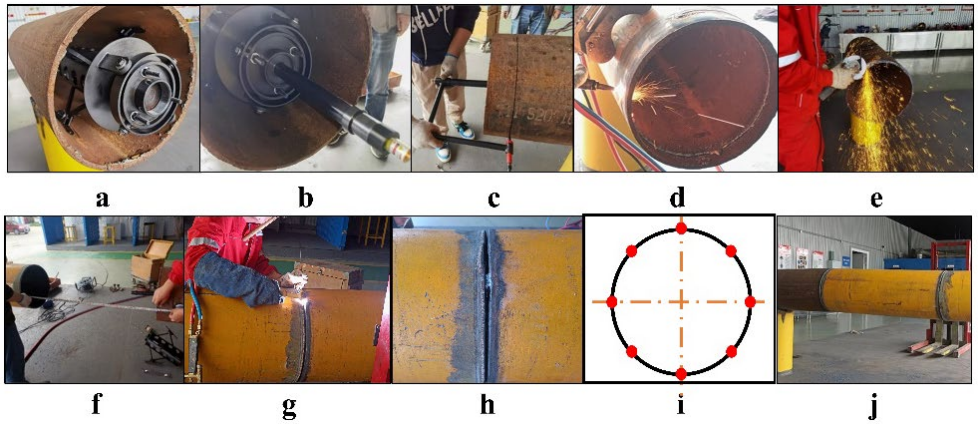

Fig. 13. Experimental flow chart

Use a gas welding cutter to cut the pipe along the traced line, as depicted in Fig. 13(d). After the cutting process, the end face of the pipe has metal burn residues. To remove these, use a handheld grinder for polishing, as illustrated in Fig. 13(e). To ensure the cutting accuracy meets the requirements, conduct a manual re-inspection. The distances between the corresponding points on the circumferences of both pipe end faces are identical, each being 1100mm, which aligns with the expected requirements, as shown in Fig. 13(f). Take a cylindrical pipe with a length of 1100mm, and fix the pipe through spot welding, as shown in Fig. 13(g). The width of the weld at the cross-section of the pipe is as shown in Fig. 13(h). According to the work experience of the on-site workers,find 8 points evenly distributed in the circumferential direction of the pipe, as shown in Fig. 13(i). The measured data of the weld width is as shown in Table 5, By analyzing the data in the table, it is known that the weld width is within the range of 0.94mm-2mm. The maximum weld width that can be welded on site is 3mm, which meets the on-site experimental standards.Finally, perform weld repair work on the pipe, and the final welding effect is as shown in Fig. 13(j).

Table 4

Table of the operation time

Group	1	2	3	4	5
Duration(s)	412	304	294	286	275

Table 5

Table of the Weld Seam Width

Group	**1**	**2**	**3**	**4**	**5**	**6**	**7**	**8**
Width(mm)	0.94	1.67	1.54	1.20	2.00	1.87	1.55	1.82

5. Conclusions

(1)Based on previous research, this paper carries out the structural design and experimental analysis of new pipeline repair equipment.

(2)This paper establishes the theoretical model of new pipeline repair equipment. It is specifically for two DN400 pipelines with non-overlapping axes, and the theoretical model is completely valid when the angle between the axes is within 10°. This article calculates the structural parameters of new pipeline repair equipment and conducts finite element simulation analysis on the key components of the equipment. The structure is optimal when the connecting rod length is designed to be 190mm.

(3)This paper conducts field experiments on the new pipeline repair equipment. The equipment's fixation work, long-distance docking work and marking lines work can be completed within 5 minutes, and the error does not exceed 2mm. The marking lines time and the precision of the cutting butt joint can meet the requirements of field operations.

REFERENCES

[1]. *Dan Ye, Yi Qu.* "Comptation model and operation method for tie-in of long-distance pipeline", in Oil and Gas Storage and Transportation, **vol. 12,** no. 36,2017, pp. 1414-1418.

[2]. *Luo, Z.; Li, Y.; Zhang, H.* "Experimental and Simulation Studies of Micro-Swing Arc Wel ding Process for X80M Pipeline", in Metals, no.13, 2023, pp.1228.

[3]. *Patrick G.* "State-of-the-Art Review of Performance Objectives for Legacy Gas Pipelines with Pipe-in-Pipe Rehabilitation Technologies", in Journal of Pipeline Systems Engineering and Practice, **vol. 14,** no.2, 2023, pp. 1-13.

[4]. *Xinhui Wang.* "Simulation Analysis of External Damage and Repair of the Gas Transmission Pipeline", in Advances in Materials Science and Engineering, **Vol.20**,2022. pp.23-26.

[5]. *Fan, Tao.* "Development of cost-effective repair system for locally damaged long-distance oil pipelines", in CONSTRUCTION AND BUILDING MATERIA, **Vol.333**,2022, pp.132.

[6]. *Caineng Zou,Qun Zhao,Jianjun Chen.* "Natural gas in China: Development trend and strategic forecast",in Natural Gas Industry B,2018,**Vol.5**,no.4,2018,pp. 380-390.

[7]. *Yang Zhang.* "Rush repair and maintenance technology of long distance natural gas pipeline",in Petrochemical Technology, **Vol.29,**no.2,2022, pp.82-83.

[8]. *Liu, XQ.* "Multi-level optimization of maintenance plan for natural gas pipeline systems subject to external corrosion",in Journal of Natural Gas Science and Engineering,**Vol.50**,2018,pp.64-73.

[9]. *Li, XH.* "Optimal maintenance strategy for corroded subsea pipelines(Article",in Journal of Loss Prevention in the Process Industries,**Vol.49**,2017,pp.145-154.

[10]. *Wei Qin.*"Calculation and placement of in-plane pipeline round-trip bends ",in Chemical Management ,**Vol.20**,2015,pp.72-73.

[11]. *Lin Fan;Huai Su.* "Supply reliability-driven joint optimization of maintenance and spare parts inventory in a gas pipeline system",in Gas Science and Engineering,**Vol.110**,2023,pp.20-43.

[12]. *Eo, Cheolwon;Yoon, Shikyung;Lee, Jong Min.* "Analysis of the effect of pipe rupture on adjacent pipes using CFD",in Journal of Loss Prevention in the Process Industries,**Vol.75**,2022,pp.14-25.

[13]. *Guangqing MEI, Jing WEI, CHEN Shuang.* "Application of new pipeline connector rapid discharging equipment in oil and gas pipeline construction",in Journal of Oil and Gas, 2014,pp.258-259.

[14]. *Lu, Hongfang.* "Trenchless Construction Technologies for Oil and Gas Pipelines: State-of-the-Art Review",in Journal of Construction Engineering & Management,**Vol. 146**,no.6,2020,pp.1-21.

[15]. *Kaituo Jiao*. "Study on the multi-objective optimization of reliability and operating cost for natural gas pipeline network",in Oil & Gas Science and Technology,**Vol.76**,2021,pp.42-64.